Large-area broad band saturable Bragg reflectors using oxidized AlAs in the circular and inverted mesa geometries

Sheila P. Nabanja, Leslie A. Kolodziejski, Gale S. Petrich, Michelle Y. Sander, Jonathan L. Morse, Katia Shtyrkova, Erich P. Ippen, and Franz X. Kärtner

Citation: Journal of Applied Physics **113**, 163102 (2013); doi: 10.1063/1.4802694
View online: https://doi.org/10.1063/1.4802694
View Table of Contents: http://aip.scitation.org/toc/jap/113/16
Published by the American Institute of Physics

Large-area broad band saturable Bragg reflectors using oxidized AlAs in the circular and inverted mesa geometries

Sheila P. Nabanja,[1,a)] Leslie A. Kolodziejski,[1] Gale S. Petrich,[1] Michelle Y. Sander,[2] Jonathan L. Morse,[1] Katia Shtyrkova,[1] Erich P. Ippen,[1] and Franz X. Kärtner[1]
[1]*Massachusetts Institute of Technology, 77 Massachusetts Avenue, Cambridge, Massachusetts 02139, USA*
[2]*Boston University, 8 St. Mary's Street, Boston, Massachusetts 02215, USA*

(Received 10 January 2013; accepted 9 April 2013; published online 25 April 2013)

A semiconductor Saturable Bragg Reflector (SBR) is a mirror structure comprising alternating layers of high and low refractive index materials with an incorporated saturable absorber. SBRs can be used to initiate and sustain ultra-short pulses in various laser systems. In order to form ultra-short pulses, SBRs with high reflectivity over a broad wavelength range are required. Furthermore, large-area SBRs facilitate easy integration in a laser cavity. One of the key elements for the realization of broad band SBRs is the development of the thermal oxidation process that creates buried low-index Al_xO_y layers over large areas. The design, fabrication, characterization, and implementation of broad band, high index contrast III-V/Al_xO_y SBRs in the form of circular mesas, as well as inverted mesa structures, is presented. [http://dx.doi.org/10.1063/1.4802694]

I. INTRODUCTION

The thermal oxidation of $Al_xGa_{1-x}As$ with high Al content ($x > 0.85$)[1] is an enabling technology in the fabrication of optoelectronic, electronic, and photonic devices such as edge-emitting lasers,[2] vertical cavity surface emitting lasers (VCSELs),[3] metal semiconductor field effect transistors (MESFETs) that are based on GaAs,[4] as well as III/V-oxide broad band Saturable Bragg Reflectors (SBRs). The low refractive index of Al_xO_y, the stable oxide that is created by thermal oxidation, makes Al_xO_y extremely useful in applications where a high index contrast is required. In the majority of the work that has been reported to date, the oxidation of Al-based materials occurred in relatively small areas. In the oxidation of VCSELs for the formation of oxide apertures,[1–4] the oxide extent does not have to exceed a few tens of microns in order to satisfy the purposes of current and optical confinement. In contrast, the wet thermal oxidation of the large-area SBRs extends over hundreds of microns.

SBRs can be used as the primary mode-locking element, or as the starting mechanism for soliton mode-locked fiber lasers and solid state Kerr-Lens mode-locked (KLM) systems.[6] With an absorber to initiate pulsing, the critical cavity alignment that is otherwise required for Kerr lens mode-locking is relaxed.[7,8] Typically, in standard SBRs, the absorbers are integrated onto AlGaAs/GaAs Bragg mirrors, and the low-index contrast ($\Delta n \sim 0.5$–0.6) between the layers results in narrow bandwidth mirrors (~70 nm, $R > 99.5\%$). This paper focuses on the development of large-area SBRs, which use high index contrast ($\Delta n \sim 1.8$) Bragg mirrors to achieve high reflectivity over a broad wavelength range for the realization of a laser that is widely tunable and that is capable of femtosecond pulses. Fig. 1 summarizes the tuning results that have been obtained using a broad band oxidized SBR, which contained 7 pairs of $Al_{0.19}Ga_{0.81}As/Al_xO_y$ as the Bragg stack and a 6 nm thick strained $In_{0.14}Ga_{0.86}As$ quantum well (sandwiched between $Al_{0.19}Ga_{0.81}As$ barriers) as the absorber section to mode-lock a Cr:LiSAF laser. Continuous tuning over 105 nm was achieved, the broadest tuning range that has been reported from any SBR mode-locked femtosecond solid state laser.

At the core of broad band SBRs is the stable conversion of AlAs to lower index Al_xO_y via lateral wet oxidation.[9–17] In order to ensure process controllability, a physical model for the oxidation of SBRs has been developed. The rate of oxidation is found to be dependent not only on the oxidation temperature but also on oxidation time, mesa geometry, and AlAs layer thickness. Using the model, the first Inverted Mesa SBR (IMSBR) that is centered at 1550 nm has been

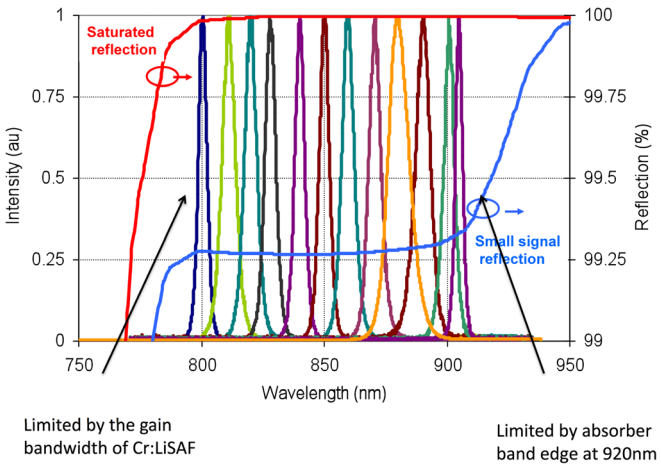

FIG. 1. Optical spectra from the tunable Cr:LiSAF laser with an oxidized SBR. A broad band tuning range of over 105 nm is achieved. Small signal and saturated reflectivity of the oxidized SBR are also shown.[5]

[a)]Author to whom correspondence should be addressed. Electronic mail: snabanja@alum.mit.edu

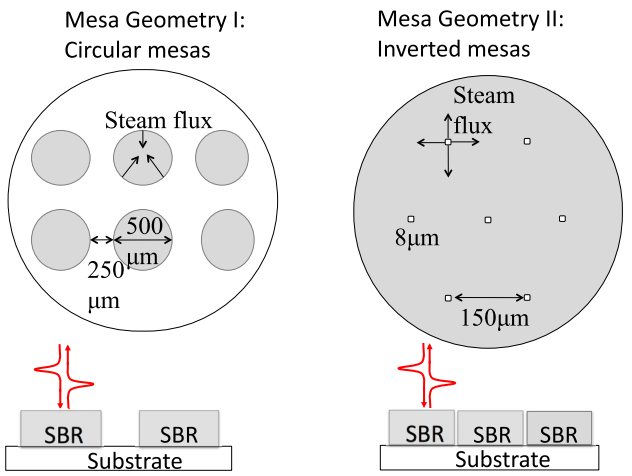

FIG. 2. Mesa layouts showing 500 μm-diameter circular mesas, as well as 8 μm aperture arrays that form the inverted structure.

designed, fabricated, characterized, and implemented in a laser cavity. IMSBRs have the advantage of easier beam alignment as compared to the previously demonstrated 500 μm-diameter circular oxidized SBRs.[9] As illustrated in Fig. 2, 99% of the surface area on an inverted structure is usable as a SBR.

II. EXPERIMENTAL PROCEDURE

A. Design

A semiconductor-based SBR consists of a saturable absorber that is integrated on a Distributed Bragg Reflector (DBR), which is formed by growing multiple layers of alternating indices of refraction such that each layer boundary causes a partial reflection of the incident optical wave. The saturable absorber initiates and sustains mode-locking by introducing an intensity-dependent loss in the laser cavity. Each SBR is uniquely designed to meet the mode-locking requirements of the laser in which it is to be implemented. A well-designed SBR must meet the following criteria:

- The absorber can be integrated onto the DBR.
- The absorber material of choice features saturable absorption at the laser wavelength.
- The device structure and materials selection enables the choice of key parameters such as recovery times and saturation fluence.
- The SBR has low insertion loss.
- The SBR has a large enough incident area so as to mitigate the heating effects of two-photon absorption. Thermally conductive packaging can also be used to conduct heat away during operation.

B. Fabrication

Large-area, wet oxidation of $Al_xGa_{1-x}As$ SBR structures is a relatively straight-forward process that involves exposing high Al-content layers to water vapor in an inert environment at elevated temperatures. The oxidation system that was used incorporates a water vapor source and a 2-in.-diameter single zone quartz tube furnace. The water vapor is supplied by bubbling N_2 through a flask of de-ionized water, which is immersed in a water bath that is maintained at 85 °C. The water vapor is carried by N_2 gas from the bubbler into the heated furnace. The oxidation temperature was varied between 420 °C and 450 °C.

The as-grown oxidizable SBR structures consist of a seven-pair GaAs/AlAs Distributed Bragg Reflector and a 60 nm thick $In_{0.53}Ga_{0.47}As$ absorber that is clad by GaAs. The structure was grown by Molecular Beam Epitaxy (MBE) on GaAs (100) substrates. Mesas were patterned immediately before oxidation by using photolithography followed by a wet etch that is comprised H_2SO_4:H_2O_2:H_2O in a 1:8:40 ratio, respectively. Oxidation begins at the exposed mesa edge and proceeds inwards by 250 μm for full oxidation of the 500 μm-diameter mesas and ~80μm in the inverted structures as shown in Fig. 2. At elevated temperatures, aluminum atoms readily react with water molecules to form Al_xO_y. The oxidation process is not reaction-rate limited, but rather, is limited by the ability with which the oxidant can diffuse across the already-formed oxide to the buried AlAs [stage 2].

III. RESULTS AND DISCUSSION

Complete oxidation was achieved for SBRs at a center wavelength of $\lambda_o = 1550$ nm. Figs. 3(a) and 3(b) show a

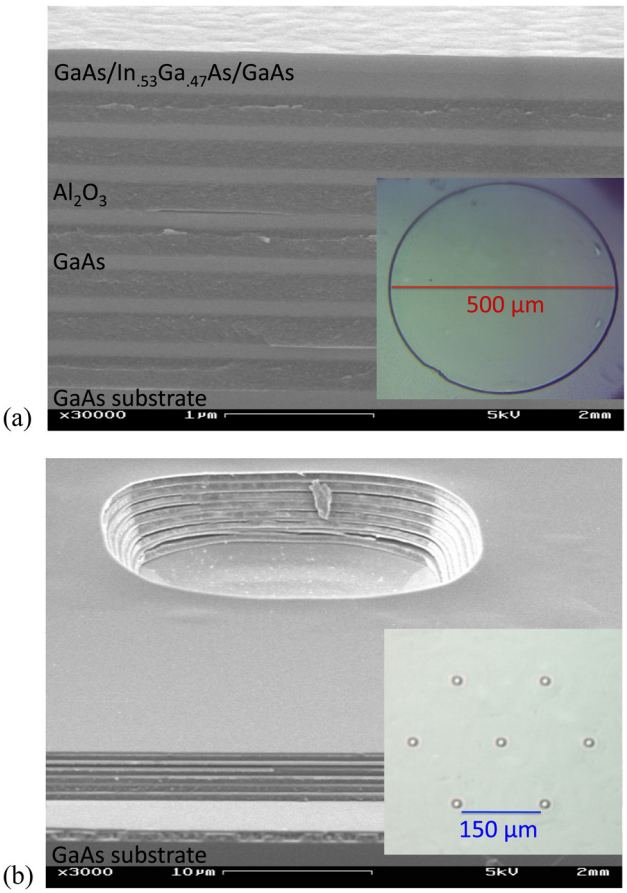

FIG. 3. Cross-sectional scanning electron microscope images of (a) a fully oxidized 500 μm-diameter circular SBR [Inset: plan-view of the mesa], and (b) a fully oxidized inverted SBR [Inset: plan-view of a unit cell of the inverted array] with a 150 μm center-to-center aperture spacing.

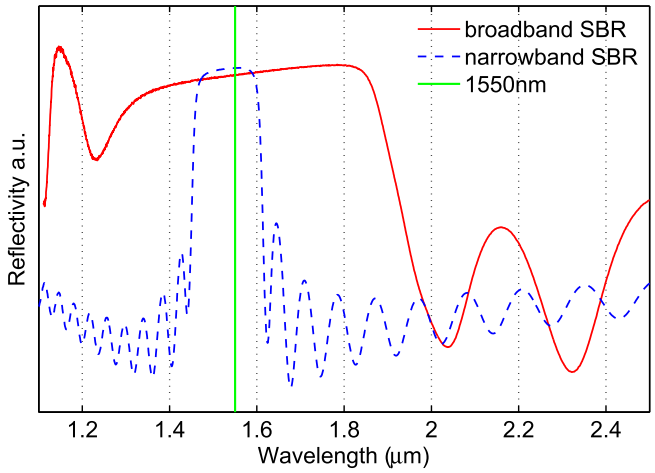

FIG. 4. Fourier Transform Infrared (FTIR) spectroscopy measurement of a narrow band GaAs/AlAs SBR versus a broad band GaAs/Al_xO_y SBR for a 1550 nm laser. The broad bandwidth in the oxidized SBRs is due to the increased index contrast of the Bragg mirror.

fully oxidized circular SBR mesa and an inverted mesa structure, respectively, that were designed to mode-lock an Erbium-doped fiber laser. $In_{0.53}Ga_{0.47}As$ served as the saturable absorber layer for 1550 nm. The SEM image in Fig. 3(a) indicates the conversion of AlAs to Al_xO_y by the distinct polycrystalline/single crystal nature of the oxidized SBR layered structure.

The motivation for developing Al(Ga)As/Al_xO_y SBRs is the increase in the high reflectivity bandwidth. In Fig. 4, the bandwidth of the GaAs/Al_xO_y SBR is much broader (approximately four times) than in the Al(Ga)As/GaAs SBR. The reflectivity spectra in Fig. 4 also reveal a slight linear absorption loss that originates from the absorber layer in both the broad band and the narrow band AlGaAs/GaAs SBRs.

The reflectivities from the circular SBRs, as well as IMSBR devices have been measured. Fig. 5 shows that the measured reflectivities from the circular SBR and IMSBR devices agree very well with the theoretical reflectivity, as well as with each other, confirming that the reflectivity of the fully fabricated devices is independent of the device geometry since the layers are identical. All three curves reveal

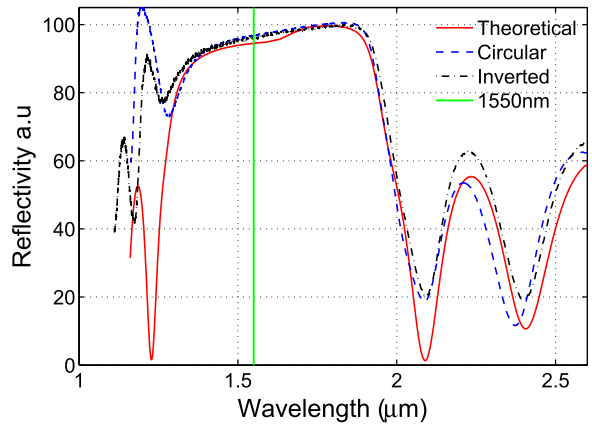

FIG. 5. Theoretical and FTIR reflectivity plots of the circular SBR and IMSBR devices that are centered at λ_o = 1550 nm showing the broad reflection bandwidth of the oxidized SBRs.

broad reflectivity bandwidths of ~600 nm with saturable losses originating from the absorber layer.

The circular SBRs were incorporated into a free-space section of a soliton mode-locked, free space lens coupled Er-doped fiber laser. Steady mode-locking was initiated using the circular SBRs at a threshold 980 nm wavelength pump power of 270 mW, and was maintained as the pump power was increased to ~415 mW. Fig. 6 is an optical spectral analyzer (OSA) trace of the laser's output spectrum at a pump power of 400 mW, showing a 3-dB spectral bandwidth of 8.4 nm, which corresponds to a transform-limited pulse duration of 296 fs. The laser's fundamental repetition rate was 314 MHz [Fig. 6, inset], which is determined by the length of the laser cavity. A wide span RF trace [not pictured] showed equal amplitude of the fundamental frequency and its harmonics, thus, demonstrating that the laser was in single pulse mode-locking operation. In this fiber laser, the full broad bandwidth of the SBR could not be fully demonstrated as the spectral bandwidth is mostly determined by the balance of the dispersion and self-phase modulation. Additionally, continuous broad band mode-locking tunability is possible by the use of oxidized SBRs and would be limited only by the location of the absorber band edge and the gain bandwidth of the laser.

Similar mode-locking results using IMSBRs have been demonstrated at a pump power of 275 mW and were maintained as the pump power was increased to ~490 mW. Fig. 7 is an OSA trace of the laser's output spectrum at a pump power of 490 mW, showing a 3-dB spectral bandwidth of 7.5 nm, which corresponds to a transform-limited pulse duration of 336 fs. The laser's fundamental repetition rate was 312 MHz [Fig. 7, inset]. The easier alignment of the laser to virtually anywhere on the SBR, rather than specific mesa sections, makes IMSBRs more practical for integration in real-world ultrafast lasers.

As part of the investigation of possible limitations to the implementation of oxidized SBRs, the non-saturable losses of the SBR were measured. Non-saturable losses, which are

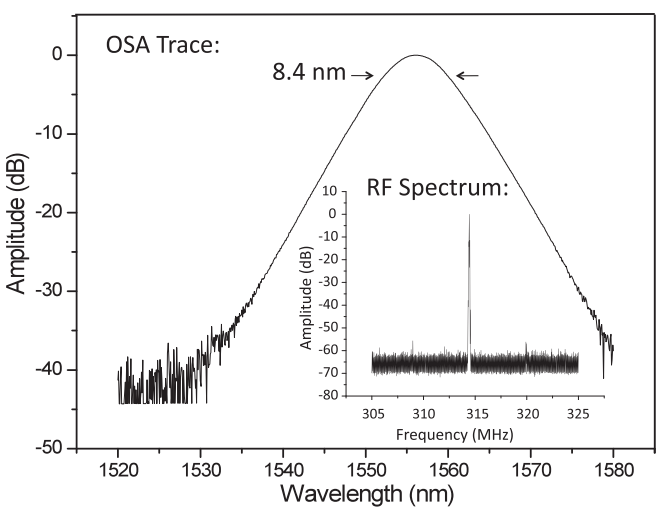

FIG. 6. OSA trace of a mode-locked laser pulse that is centered at λ_o = 1555 nm with a 3-dB spectral bandwidth of 8.4 nm and inset: a repetition rate of 314 MHz using the oxidized circular mesa SBRs.

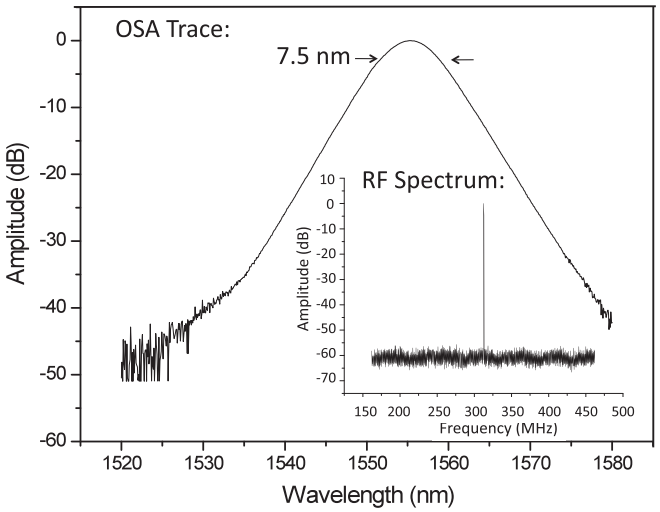

FIG. 7. OSA trace of a mode-locked pulse that is centered at $\lambda_o = 1556$ nm with a 3-dB bandwidth of 7.5 nm and inset: a repetition rate of 312 MHz using the oxidized IMSBRs.

typically undesirable and do not contribute to mode-locking, are caused by absorption of the optical signal by the Bragg mirror, or by scattering from rough surfaces. The non-saturable losses were quantified using a three-part experiment whereby the reflectivity of pulses that were emitted from a Ti:sapphire-pumped optical parametric oscillator were measured as a function of fluence. The pulse parameters were: pulsewidth = 180 fs, $\lambda_o = 1550$ nm, and repetition rate = 80 MHz. The oxidized SBRs were moved in and out of the focal plane of the incident optical signal by a small distance, and a reflectivity trace was taken in each position. The results that are shown in Fig. 8 show data for traces at 9.5, 10, 10.5, and 11 mm from the focussing lens that precedes the SBR.

For fluences above saturation, a maximum reflectance of ~98% relative to an AlGaAs/GaAs dielectric mirror was measured for the SBR mesa at 9.5 mm from the lens. This result estimates a non-saturable loss of ~2%. The small non-saturable loss of the fabricated broad band oxidized SBRs makes them a good candidate for ultrafast pulse generation.

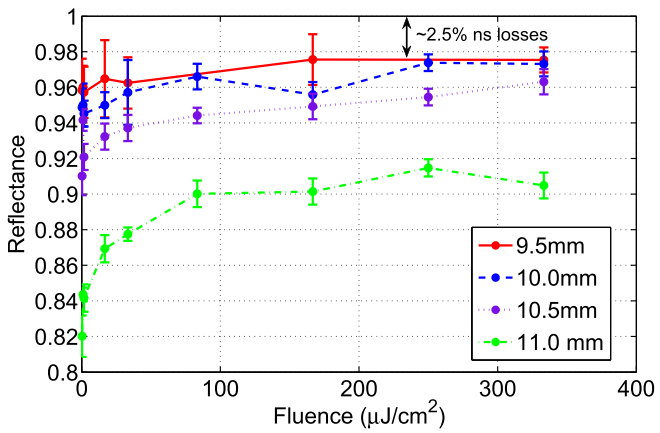

FIG. 8. Reflectance traces from an oxidized circular mesa as the fluence is increased at four positions. A non-saturable loss of ~2.5% is recorded 9.5 mm away from the focussing lens.

IV. CONCLUSIONS

IMSBRs, which enable the generation of widely tunable ultra-short pulses, have been developed. In addition to possessing broad reflectivity bandwidths, large-area IMSBRs facilitate easier beam alignment as compared to circular SBRs, making them especially attractive for the implementation in real-world ultrafast lasers. Optical characterization shows similar mode-locking performance in the circular mesa and inverted geometries. Currently, the inverted mesa approach is being extended to the development of IMSBRs at various wavelengths, where other broad band laser materials are available.

ACKNOWLEDGMENTS

The authors wish to acknowledge Dr. Umit Demirbas for the design and testing of the Cr:LiSAF-based SBRs, and Dr. Hyunil Byun for developing the initial Erbium-doped fiber laser cavity.

[1]K. D. Choquette, K. M. Geib, C. H. Ashby, R. D. Twesten, O. Blum, H. Q. Hou, D. M. Follstaedt, E. E. Hammons, D. Mathes, and R. Hull, "Advances in selective wet oxidation of AlGaAs alloys," IEEE J. Quantum Electron. **3**, 916–926 (1997).
[2]F. A. Fish, S. J. Caracci, N. Holonyak, J. M. Dallesasse, K. C. Hsieh, and M. J. Ries, "Planar native-oxide index guided AlGaAs GaAs quantum well heterostructure lasers," Appl. Phys. Lett. **39**, 1722–1757 (1991).
[3]M. S. Wu, G. S. Li, W. Yuen, and C. J. Chang-Hasnain, "Widely-tunable 1.5 μm micromechanical optical filter using Al_xO_y/AlGaAs DBR," Electron. Lett. **33**, 1702–1703 (1997).
[4]P. A. Parikh, P. M. Chavakar, and U. K. Mishra, "GaAs MESFET's on a truly insulating buffer layer: Demonstration of the GaAs on insulator technology," IEEE Electron Device Lett. **18**, 111–113 (1997).
[5]U. Demirbas, G. S. Petrich, S. Nabanja, J. R. Birge, L. A. Kolodziejski, F. X. Kaertner, and J. G. Fujimoto, "Widely-tunable femtosecond operation of Cr:LiSAF lasers using broadband saturable Bragg reflectors," in Conference on Lasers and Electro-Optics (2010).
[6]D. H. Sutter, G. Steinmeyer, L. Gallmann, N. Matuschek, F. Morier-Genoud, U. Keller, V. Scheuer, G. Angelow, and T. Tschudi, "Semiconductor saturable-absorber mirror assisted Kerr-lens mode-locked Ti:sapphire laser producing pulses in the two-cycle regime," Opt. Lett. **24**, 631–633 (1999).
[7]U. Keller, K. Weingarten, F. X. Kaertner, D. Kopf, and I. D. Jung, "Semiconductor saturable absorber mirrors (SESAMs) for femtosecond to nanosecond pulse generation in solid-state lasers," IEEE J. Sel. Top. Quantum Electron. **2**, 435–453 (1996).
[8]S. Tsuda, W. H. Knox, E. A. deSouza, W. Y. Jan, and J. E. Cunningham, "Low-loss intracavity AlAs/AlGaAs saturable Bragg reflector for femtosecond mode locking in solid-state lasers," Opt. Lett. **20**, 1406–1408 (1995).
[9]S. N. Tandon, J. T. Gopinath, H. M. Shen, G. S. Petrich, L. A. Kolodziejski, F. X. Kaertner, and E. P. Ippen, "Large-area broadband saturable Bragg reflectors by use of oxidized AlAs," Opt. Lett. **29**, 2551–2553 (2004).
[10]T. Langenfelder, S. Schroder, and H. Grothe, "Lateral oxidation of AlGaAs layers in a wet ambient," Appl. Phys. Lett. **82**, 3548–3551 (1997).
[11]T. Yoshikawa, H. Saito, H. Kosaka, Y. Sugimoto, and K. Kasahara, "Self-stopping selective oxidation process of AlAs," Appl. Phys. Lett. **72**, 2310–2312 (1998).
[12]M. Ochiai, G. E. Giudice, H. Temkin, J. W. Scott, and T. M. Cockerill, "Kinetics of thermal oxidation of AlAs in water vapor," Appl. Phys. Lett. **68**, 1898–1900 (1996).
[13]B. Koley, M. Dagenais, M. R. Jin, J. Pham, G. Simonis, G. McLane, and D. Stone, "Kinetics of growth of AlAs oxide in selectively oxidized vertical cavity surface emitting lasers," J. Appl. Phys. **82**, 4586–4589 (1997).
[14]B. Koley, M. Dagenais, M. R. Jin, J. Pham, G. Simonis, G. McLane, F. Johnson, and R. Whaley, Jr., "Dependence of lateral oxidation rate on

thickness of AlAs layer of interest as a current aperture in vertical-cavity surface-emitting laser structures," J. Appl. Phys. **84**, 600–605 (1998).
[15]M. Osinski, T. Svimonishvili, G. A. Smolyakov, V. A. Smagley, W. Mackowiak, "Temperature and thickness dependence of steam oxidation of AlAs in cylindrical mesa structures," IEEE Photon. Technol. Lett. **13**, 687–697 (2001).
[16]P. C. Ku, J. A. Hernandez, and C. J. Chang-Hasnain, "Buried selectively-oxidized AlGaAs structures grown on nonplanar substrates," Opt. Express **10**, 1003–1008 (2002).
[17]P. C. Ku and C. J. Chang-Hasnain, "Thermal oxidation of AlGaAs: Modeling and process control," IEEE J. Quantum Electron. **39**, 577–585 (2003).